

Reinforcement Learning for Safety-Critical Control under Model Uncertainty, using Control Lyapunov Functions and Control Barrier Functions

Jason Choi^{*1}, Fernando Castañeda^{*1}, Claire J. Tomlin², Koushil Sreenath¹

Abstract—In this paper, the issue of model uncertainty in safety-critical control is addressed with a data-driven approach. For this purpose, we utilize a structure of an input-output linearization controller based on a nominal model, and Control Barrier Function (CBF) and Control Lyapunov Function (CLF)-based control methods. Specifically, a novel Reinforcement Learning framework which learns the model uncertainty in CBF and CLF constraints, as well as other dynamic constraints is proposed. The trained policy is combined with the nominal model-based CBF-CLF-QP, resulting in the *Reinforcement Learning based CBF-CLF-QP (RL-CBF-CLF-QP)*, which now addresses the problem of uncertainty in the safety constraints. The performance of the proposed method is validated by testing it on an underactuated nonlinear bipedal robot walking on randomly spaced stepping stones with one step preview.

I. INTRODUCTION

In this work, we address the issue of model uncertainty in safety-critical control using a data-driven machine learning approach. Our goal is to benefit from the recent successes of learning-based control in highly uncertain dynamical systems, such as in Hwangbo et al. [10] and Levine et al. [11], yet to also account for safety in a formal way. We seek to combine the benefits of these data-driven approaches, with the benefits of classical model-based control methods which have theoretical guarantees on stability and safety. Towards this, we use Control Lyapunov Function (CLF) and Control Barrier Function (CBF)-based controllers designed on nominal systems that are then trained to work on systems with uncertainty through reinforcement learning (RL).

A. Related Work

In the field of controls, Control Lyapunov Function (CLF)-based and Control Barrier Function (CBF)-based control methods have been shown to be successful for safety-critical control. Galloway et al. [8] and Ames and Powell [1] have shown that CLF-based quadratic programs (CLF-QP) with constraints can be solved online for performing locomotion and manipulation tasks. In Ames et al. [3], CBFs have been incorporated with the CLF-QP, namely CBF-CLF-QP, to handle safety constraints effectively in real time.

These CLF-based and CBF-based methods heavily rely on accurate knowledge of the system model, which gives rise to adaptive or robust versions. In Nguyen and Sreenath [13], an L_1 adaptive controller has been incorporated with CLF-QP in order to adapt to model uncertainty, and has been demonstrated for bipedal walking. In Nguyen and Sreenath [12], a robust version of the CBF-CLF-QP has been proposed, that solves the quadratic program for the worst case effect of model uncertainty. While these methods can tackle model uncertainty to some degree, it may often fail to account for the correct magnitudes of adaptation and uncertainty.

Recently, several works addressing the issue of model uncertainty in the control problem using a data-driven approach have been proposed. Westenbroek et al. [19] has proposed a RL-based method to learn the model uncertainty compensation for input-output linearization control. Taylor et al. [17] and Taylor et al. [18] each addresses how to learn the uncertainty in CLF and CBF constraints respectively, using an empirical risk minimization. Our methodologies most closely align with these works in that we are also explicitly dealing with learning to reduce model uncertainty in input-output linearization, CLF, and CBF-based control. However, the main difference in our approach is that we have devised a unified RL-based framework for learning model uncertainty in CLF, CBF, and other dynamic safety constraints altogether in a single learning process. In addition to the aforementioned works, there are also a few (Bansal et al. [4], Fisac et al. [7], Berkenkamp et al. [5]) that learn model uncertainty through probabilistic models such as Gaussian Processes. These approaches allow analysis of the learned model or policy, however they can scale poorly with state dimension, and therefore present a challenge for high order systems.

B. Contributions

In this paper, we present a novel RL-based framework which combines two key components: 1) an RL agent which learns model uncertainty in multiple general safety constraints, including CLF and CBF constraints, through training, and 2) a quadratic program that solves for the control that satisfies the safety constraints under the learned model uncertainty. We name this framework **Reinforcement Learning based CBF and CLF Quadratic Program (RL-CBF-CLF-QP)**. After training, the RL-CBF-CLF-QP can be executed online with fast computation. The overall diagram of our framework is presented in Fig. 1. Here is the summary of the contribution

* Indicates equal contribution.

¹ UC Berkeley, Mechanical Engineering.

² UC Berkeley, Electrical Engineering and Computer Sciences.

The work of Jason Choi received the support of a fellowship from Kwanjeong Educational Foundation, Korea. The work of Fernando Castañeda received the support of a fellowship (code LCF/BQ/AA17/11610009) from la Caixa Foundation (ID 100010434). This work was partially supported through National Science Foundation Grant CMMI-1931853.

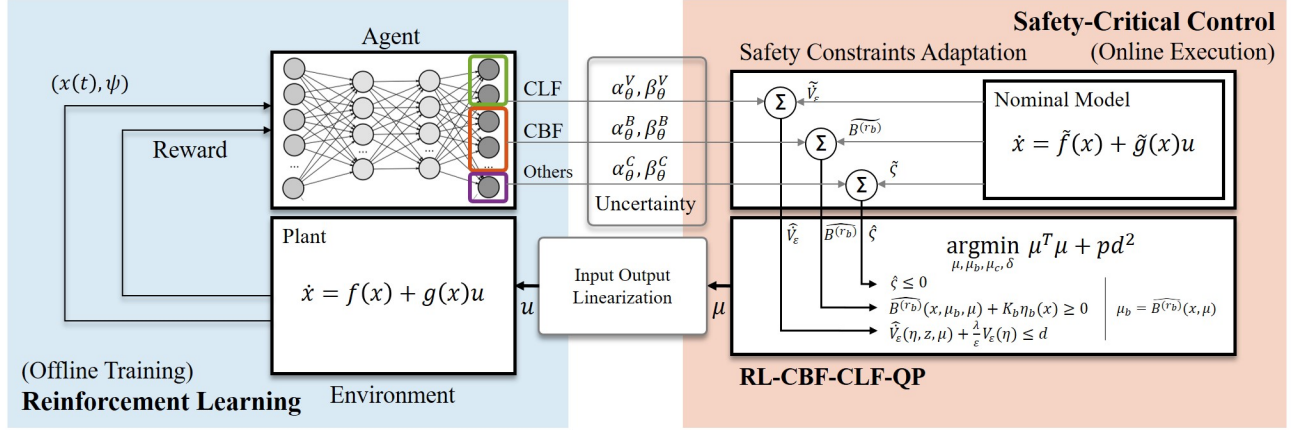


Fig. 1: Our method (RL-CBF-CLF-QP): **Reinforcement Learning**: An RL agent learns model uncertainty in multiple general safety constraints including CLF and CBF constraints through training. **RL-CBF-CLF-QP**: the combination of learned uncertainty terms and safety constraints derived from a nominal model results in the estimate of the true plant safety constraints, and the quadratic program that satisfies the estimated safety constraints solves for the control input.

of our work:

- 1) We present a reinforcement learning framework that learns model uncertainty for CLF, CBF, and other dynamic constraints in a single learning process.
- 2) We generalize our method to high relative-degree outputs as well as Control Barrier Functions.
- 3) Our method can learn the uncertainty in the dynamics of parameterized CBFs that are not only state-dependent but also dependent on other parameters.
- 4) We numerically validate our method on an underactuated nonlinear hybrid system, such as a bipedal robot walking on stepping stones with significant model uncertainty.

C. Organization

In Section II, we briefly explain the necessary background for the paper. In Section III, we discuss how we can learn model uncertainty in the CLF constraint for CLF-QP through RL. In Section IV, we expand this method to learn uncertainties in CBF and general dynamic constraints, and propose the RL-CBF-CLF-QP. In Section V, we discuss how the RL agent can learn aforementioned uncertainties. In Section VI, VII, we provide and explain the results of the demonstration of RL-CBF-CLF-QP for a bipedal robot. Finally, we discuss about the limitation of our method in Section VIII and give concluding remarks in Section IX.

II. BACKGROUND

A. Input-Output Linearization

Considering a control affine nonlinear system

$$\begin{aligned} \dot{x} &= f(x) + g(x)u, \\ y &= h(x), \end{aligned} \quad (1)$$

with $x \in \mathbb{R}^n$ being the system state, $u \in \mathbb{R}^m$ the control inputs and $y \in \mathbb{R}^m$ the outputs of the system, assuming there are the same number of outputs as inputs. We make the standard assumption that the vector fields f and g are Lipschitz

continuous. Then, if the vector relative degree of the outputs is r , we have

$$y^{(r)} = L_f^r h(x) + L_g L_f^{r-1} h(x)u, \quad (2)$$

where the functions $L_f^r h$ and $L_g L_f^{r-1} h$ are known as r^{th} order Lie derivatives. More information about Lie derivatives can be found in Sastry [15]. Here, $y^{(r)}$ is the vector of r^{th} derivatives of each output in y , and (2) indicates that the inputs u first appear at the r^{th} derivative of these outputs, and not for lower derivatives. If $L_g L_f^{r-1} h \neq \mathbf{0}$ and nonsingular $\forall x \in D$, with $D \subset \mathbb{R}^n$ being a compact subset containing the origin, then we can apply a control input which renders the input-output dynamics of the system linear:

$$u(x, \mu) = u^*(x) + \left(L_g L_f^{r-1} h(x) \right)^{-1} \mu, \quad (3)$$

where u^* is the feedforward term:

$$u^*(x) = - \left(L_g L_f^{r-1} h(x) \right)^{-1} L_f^r h(x), \quad (4)$$

and μ is the auxiliary input.

Using this control law yields the input output linear system $y^{(r)} = \mu$, and we can define a state transformation $\Phi : x \rightarrow (\eta, z)$, with

$$\eta = [h(x)^\top, L_f h(x)^\top, \dots, L_f^{r-1} h(x)^\top]^\top \quad (5)$$

and $z \in Z$, where $Z = \{x \in \mathbb{R}^n \mid \eta \equiv \mathbf{0}\}$. The closed-loop dynamics of the system can then be represented as a linear time invariant system on η and the zero-dynamics on z :

$$\begin{cases} \dot{\eta} = F\eta + G\mu, \\ \dot{z} = p(\eta, z), \end{cases} \quad (6)$$

$$F = \begin{bmatrix} 0 & I_m & . & . & 0 \\ 0 & 0 & I_m & . & 0 \\ . & . & . & . & . \\ 0 & . & . & . & I_m \\ 0 & . & . & . & 0 \end{bmatrix} \quad \text{and} \quad G = \begin{bmatrix} 0 \\ . \\ . \\ 0 \\ I_m \end{bmatrix}, \quad (7)$$

with $F \in \mathbb{R}^{mr \times mr}$ and $G \in \mathbb{R}^{mr \times m}$.

B. Control Lyapunov Function Based Quadratic Programs

In Ames et al. [2] a control method that guarantees exponential stability of η with a rapid enough convergence rate is presented. It introduces the concept of *rapidly exponentially stabilizing control Lyapunov function (RES-CLF)*. Specifically, a one-parameter family of continuously differentiable functions $V_\varepsilon : \mathbb{R}^{mr} \rightarrow \mathbb{R}$ is said to be a (RES-CLF) for system (1) if there exist some constants $\gamma, c_1, c_2 > 0$ such that for all $0 < \varepsilon < 1$ and all $\eta \in \mathbb{R}^{mr}$ the following holds

$$c_1 \|\eta\|^2 \leq V_\varepsilon(\eta) \leq \frac{c_2}{\varepsilon^2} \|\eta\|^2, \quad (8)$$

$$\dot{V}_\varepsilon(\eta, \mu) + \frac{\lambda}{\varepsilon} V_\varepsilon(\eta) \leq 0. \quad (9)$$

If we define a control input μ that makes η exponentially stable, of the form:

$$\mu = \left[-\frac{1}{\varepsilon^r} K_r, \dots, -\frac{1}{\varepsilon^2} K_2, -\frac{1}{\varepsilon} K_1 \right] \eta = K \eta, \quad (10)$$

where $K \in \mathbb{R}^{m \times mr}$, then we can choose a quadratic CLF candidate

$$V_\varepsilon(\eta) = \eta^T P_\varepsilon \eta, \quad (11)$$

where P_ε is the solution of the Lyapunov Equation $A^T P_\varepsilon + P_\varepsilon A = -Q$, with A being the closed-loop dynamics matrix $A = F + GK$ and Q any symmetric positive-definite matrix. Defining $\bar{f} = F\eta$, $\bar{g} = G$, we can write the derivative of the CLF candidate as:

$$\dot{V}_\varepsilon(\eta, \mu) = L_{\bar{f}} V_\varepsilon(\eta) + L_{\bar{g}} V_\varepsilon(\eta) \mu, \quad (12)$$

with

$$\begin{aligned} L_{\bar{f}} V_\varepsilon(\eta) &= \eta^T (F^T P_\varepsilon + P_\varepsilon F) \eta, \\ L_{\bar{g}} V_\varepsilon(\eta) &= 2\eta^T P_\varepsilon G. \end{aligned} \quad (13)$$

We can then define for every time step an optimization problem in which condition (9) becomes a linear constraint on the control input μ . The objective function can be set to minimize the norm of the control inputs, in which case the optimization problem is a quadratic program (QP):

CLF-QP:

$$\mu^*(x) = \underset{\mu}{\operatorname{argmin}} \mu^T \mu \quad (14)$$

$$\text{s.t. } \dot{V}_\varepsilon(\eta, \mu) + \frac{\lambda}{\varepsilon} V_\varepsilon(\eta) \leq 0 \quad (\text{CLF})$$

C. Control Barrier Function and Control Lyapunov Function Based Quadratic Programs

In Nguyen and Sreenath [14] the concept of Exponential Control Barrier Function (ECBF) is defined. Specifically, a function $B : \mathbb{R}^m \rightarrow \mathbb{R}$ is an ECBF of relative degree r_b for the system (1) if there exists $K_b \in \mathbb{R}^{r_b \times 1}$ such that

$$\sup_{u \in U} \left[L_f^{r_b} B(x) + L_g L_f^{r_b-1} B(x) u + K_b \eta_b(x) \right] \geq 0 \quad (15)$$

for $\forall x \in \{x \in \mathbb{R}^n \mid B(x) \geq 0\}$ with

$$\eta_b(x) = \begin{bmatrix} B(x) \\ \dot{B}(x) \\ \ddot{B}(x) \\ \vdots \\ B^{(r_b-1)}(x) \end{bmatrix} = \begin{bmatrix} B(x) \\ L_f B(x) \\ L_f^2 B(x) \\ \vdots \\ L_f^{r_b-1} B(x) \end{bmatrix}, \quad (16)$$

that guarantees $B(x_0) \geq 0 \implies B(x(t)) \geq 0, \forall t \geq 0$ (Nguyen and Sreenath [14]).

We can then choose a virtual input μ_b that allows us to input-output linearize the ECBF dynamics:

$$B^{(r_b)}(x, \mu) = L_f^{r_b} B(x) + L_g L_f^{r_b-1} B(x) u(x, \mu) =: \mu_b, \quad (17)$$

with u defined in (3). We refer readers to Nguyen and Sreenath [14] for more details.

The condition in (15) then becomes choosing μ_b such that

$$\mu_b + K_b \eta_b \geq 0. \quad (18)$$

This is then added in the following QP, where safety is prioritized over stability by relaxing the CLF constraint:

CBF-CLF-QP:

$$\mu^*(x) = \underset{\mu, \mu_b, d}{\operatorname{argmin}} \mu^T \mu + p d^2$$

$$\text{s.t. } \dot{V}_\varepsilon(\eta, \mu) + \frac{\lambda}{\varepsilon} V_\varepsilon(\eta) \leq d \quad (\text{CLF})$$

$$\mu_b + K_b \eta_b \geq 0 \quad (\text{CBF})$$

$$\mu_b = B^{(r_b)}(x, \mu)$$

$$A_c(x) \mu + b_c(x) \leq 0 \quad (\text{Constraints}) \quad (19)$$

III. REINFORCEMENT LEARNING FOR CLF-QP BASED CONTROLLERS UNDER UNCERTAIN DYNAMICS

In this section, we address the issue of having a mismatch between the model and the plant dynamics, under the situation where the true plant vector fields f, g are not precisely known. Specifically, between this and the next sections we analytically examine the effects of model uncertainty on the dynamics of the CLF, CBF and other dynamic constraints. For each of these cases we will define the goal of the RL agent and the policy to be learned.

A. Reinforcement Learning for CLF-QP Based Controllers: First Approach

Let the nominal model used in the controller be

$$\dot{x} = \tilde{f}(x) + \tilde{g}(x)u. \quad (20)$$

We assume: 1) the vector fields $\tilde{f} : \mathbb{R}^n \rightarrow \mathbb{R}^n, \tilde{g} : \mathbb{R}^n \rightarrow \mathbb{R}^{n \times m}$ are Lipschitz continuous and 2) the vector relative degrees of the model and plant dynamics are the same (r). These are the standard assumptions that have been made in most of the literature (Nguyen and Sreenath [12], Taylor et al. [17] Taylor et al. [18], Westenbroek et al. [19]) to tackle the mismatch terms analytically.

The pre-control law (3) of input-output linearization computed based on the nominal model \tilde{f}, \tilde{g} has the following form

$$\tilde{u}(x, \mu) = \tilde{u}^*(x) + \left(L_{\tilde{g}} L_{\tilde{f}}^{r-1} h(x) \right)^{-1} \mu, \quad (21)$$

with a feedforward term

$$\tilde{u}^*(x) := - \left(L_{\tilde{g}} L_{\tilde{f}}^{r-1} h(x) \right)^{-1} L_{\tilde{f}}^r h(x). \quad (22)$$

Using this \tilde{u} in (2) results in the input-output dynamics

$$y^{(r)} = \mu + \Delta_1(x) + \Delta_2(x)\mu, \quad (23)$$

where

$$\begin{aligned} \Delta_1(x) &:= L_{\tilde{f}}^r h(x) - L_g L_f^{r-1} h(x) \left(L_{\tilde{g}} L_{\tilde{f}}^{r-1} h(x) \right)^{-1} L_{\tilde{f}}^r h(x), \\ \Delta_2(x) &:= L_g L_f^{r-1} h(x) \left(L_{\tilde{g}} L_{\tilde{f}}^{r-1} h(x) \right)^{-1} - I_m. \end{aligned} \quad (24)$$

The dynamics of η from (6) now becomes:

$$\dot{\eta} = (F\eta + G\Delta_1(\eta, z)) + G(I_m + \Delta_2(\eta, z))\mu. \quad (25)$$

Note that this equation is the same as (6) if the uncertainty terms are zero. Therefore, (6) can be considered as a nominal model for the true input-output dynamics (25).

For this first approach we will use RL to define an additional input whose goal is to cancel the uncertainty terms present in the input-output dynamics (25), and therefore get the input-output dynamics to behave like (6), as done in Westenbroek et al. [19]. Ideally, if this is achieved, there will not be any uncertainty terms in the CLF dynamics, since \dot{V}_ε only depends on the matrices F and G of the linear input-output dynamics.

Applying the following input to (2)

$$u(x, \mu) = \tilde{u}(x, \mu) + u_\theta(x, \mu), \quad (26)$$

with \tilde{u} as defined in (21) and with

$$u_\theta(x, \mu) := \left(L_{\tilde{g}} L_{\tilde{f}}^{r-1} h(x) \right)^{-1} (\alpha_\theta(x)\mu + \beta_\theta(x)), \quad (27)$$

yields

$$y^{(r)} = \mu + (\Delta_1(x) + \Delta_3(x)\beta_\theta(x)) + (\Delta_2(x) + \Delta_3(x)\alpha_\theta(x))\mu. \quad (28)$$

where $\Delta_3(x) := \Delta_2(x) + I_m$, and $\theta \in \Theta \subset \mathbb{R}^N$ are parameters of a neural network to be learned. We can now clearly see the goal of the RL agent for this approach: design policy α_θ and β_θ such that $y^{(r)}$ is as close as possible to μ . Thus, the time-wise reward function can be defined as

$$R(x, \mu) = -\|y^{(r)} - \mu\|_2^2. \quad (29)$$

The CLF-QP of (34) can then be solved to get μ and the final control input used is obtained by (26).

B. Reinforcement Learning for CLF-QP Based Controllers: Second Approach

The approach that has just been presented can only be used when the CLFs are defined on the input-output linearized dynamics of the system. If the full state is required, we need to use the approach that will be presented in this section.

For the next approach, we will assume that the uncertainty of the input-output dynamics (25) has not been corrected, and we will do an analysis of the impact it will have on the dynamics of the CLF.

Under the presence of uncertainty \dot{V}_ε becomes

$$\dot{V}_\varepsilon(\eta, z, \mu) = L_{\tilde{f}} V_\varepsilon(\eta, z) + L_{\tilde{g}} V_\varepsilon(\eta, z)\mu, \quad (30)$$

where

$$\begin{aligned} L_{\tilde{f}} V_\varepsilon(\eta, z) &= L_{\tilde{f}} V_\varepsilon(\eta) + \underbrace{2\eta^\top P_\varepsilon G \Delta_1(\eta, z)}_{\Delta_1^v(\eta, z)}, \\ L_{\tilde{g}} V_\varepsilon(\eta, z) &= L_{\tilde{g}} V_\varepsilon(\eta) + \underbrace{2\eta^\top P_\varepsilon G \Delta_2(\eta, z)}_{\Delta_2^v(\eta, z)}. \end{aligned} \quad (31)$$

with \tilde{f}, \tilde{g} being the nominal model input-output linearized dynamics; namely, $\tilde{V}_\varepsilon(\eta, \mu) = L_{\tilde{f}} V_\varepsilon(\eta) + L_{\tilde{g}} V_\varepsilon(\eta)\mu$.

Therefore, under uncertainty:

$$\dot{V}_\varepsilon(\eta, z, \mu) = \tilde{V}_\varepsilon(\eta, \mu) + \Delta_1^v(\eta, z) + \Delta_2^v(\eta, z)\mu. \quad (32)$$

In this second approach we will use RL to estimate the uncertainty terms in \dot{V}_ε : Δ_1^v and Δ_2^v . For this purpose, we construct an estimate

$$\hat{V}_{\varepsilon, \theta}(\eta, z, \mu) = \tilde{V}_\varepsilon(\eta, \mu) + \beta_\theta^V(\eta, z) + \alpha_\theta^V(\eta, z)\mu, \quad (33)$$

where $\theta \in \Theta \subset \mathbb{R}^N$ are again the parameters to be learned. The goal of RL is then obvious: learn policy α_θ^V and β_θ^V such that $\hat{V}_{\varepsilon, \theta}(\eta, z, \mu)$ is as close as possible to $\dot{V}_\varepsilon(\eta, z, \mu)$. Any reward function that penalizes the absolute value of the difference between those two terms can be used. More details on the specific RL implementation will be discussed in Section V.

Remark 1: It is assumed here for convenience that α^V, β^V share the same parameters but it does not need to be the case. We will keep the abbreviation that all the policy functions to be learned in this paper are sharing the same parameters.

The estimate \hat{V}_ε in (33) will then be used as our best guess of \dot{V}_ε for the optimization problem:

RL-CLF-QP:

$$\begin{aligned} \mu^*(x) &= \underset{\mu}{\operatorname{argmin}} \mu^T \mu \\ \text{s.t. } \hat{V}_{\varepsilon, \theta}(\eta, z, \mu) + \frac{\lambda}{\varepsilon} V_\varepsilon(\eta) &\leq 0 \quad (\text{RL-CLF}) \end{aligned} \quad (34)$$

Remark 2: In this paper, we have illustrated the case where CLF is applied to the linearized input-output dynamics. The readers can easily verify that this approach is actually applicable to any kind of Lipschitz continuous control affine system.

The reason why we use CLF on the linearized input-output dynamics of the system is that this way we get a systematic approach on how to compute a CLF candidate, whereas on the nonlinear system this process could be challenging.

IV. REINFORCEMENT LEARNING FOR CBF-CLF-QP BASED CONTROLLERS UNDER UNCERTAIN DYNAMICS

A. Reinforcement Learning for CBFs

Under the presence of uncertainty (17) becomes

$$\widetilde{B^{(r_b)}}(x, \mu) = L_{\tilde{f}}^{r_b} B(x) + L_{\tilde{g}} L_{\tilde{f}}^{r_b-1} B(x) \tilde{u}(x, \mu), \quad (35)$$

and the actual CBF's r^{th} derivative can be written as:

$$B^{(r_b)}(x, \mu) = \widetilde{B^{(r_b)}}(x, \mu) + \Delta_1^b(x) + \Delta_2^b(x)\mu, \quad (36)$$

where Δ_1^b, Δ_2^b are the terms derived from the model-plant mismatch. We omit analytic expressions for the conciseness of the paper, but they can be derived in a similar way as in (24).

Remark 3: When the state of the system can be represented as $x = [q, \dot{q}]^T$, as in most robotic systems, even for the case of high relative degree CBFs, the model uncertainty only affects the r_b^{th} time derivative of B , since $B^{(r_b)}$ is the only term that depends on the plant dynamics. Indeed, if any of the terms in η_b did depend on the plant dynamics, then the relative degree of the CBF would not be r_b .

Now we will present how we can estimate the uncertainty terms for the CBF and other dynamic constraints using RL.

Remark 4: The approach presented in Section III-A cannot be used here since the CBF functions depend on the full dynamics of the system, not just the input-output linearized dynamics.

We build an estimator of $B^{(r_b)}$:

$$\widehat{B^{(r_b)}}_{\theta}(x, \mu) = \widetilde{B^{(r_b)}}(x, \mu) + \beta_{\theta}^B(x) + \alpha_{\theta}^B(x)\mu, \quad (37)$$

and the goal of RL is to learn policy α_{θ}^B and β_{θ}^B such that $\widehat{B^{(r_b)}}_{\theta}$ is as close as possible to $B^{(r_b)}$.

In the case that the CBF also depends on a set of parameters $\psi \in \mathbb{R}^q$ which might not always have the same values, then we need to redefine B as $B : \mathbb{R}^{n \times q} \rightarrow \mathbb{R}$. The neural-network policy will now need to take ψ as additional inputs $\alpha_{\theta}^B : \mathbb{R}^{n \times q} \rightarrow \mathbb{R}^m, \beta_{\theta}^B : \mathbb{R}^{n \times q} \rightarrow \mathbb{R}$ and the proposed estimate of the r^{th} time derivative of B becomes:

$$\widehat{B^{(r_b)}}_{\theta}(x, \mu, \psi) = \widetilde{B^{(r_b)}}(x, \mu, \psi) + \beta_{\theta}^B(x, \psi) + \alpha_{\theta}^B(x, \psi)\mu \quad (38)$$

In order to integrate everything in a new QP we define the new virtual input of the CBF dynamics as

$$\mu_b = \widehat{B^{(r_b)}}_{\theta}. \quad (39)$$

B. Reinforcement Learning for Additional Dynamic Constraints

Now we will study the effect of uncertainty on other constraints that depend on the dynamics of the system:

$$\underbrace{A_c(x, f, g)\mu + b_c(x, f, g)}_{\zeta(x, \mu)} \leq 0. \quad (40)$$

In the presence of model mismatch we have

$$\begin{aligned} b_c(x, f, g) &= b_c(x, \tilde{f}, \tilde{g}) + \Delta_1^c(x), \\ A_c(x, f, g) &= A_c(x, \tilde{f}, \tilde{g}) + \Delta_2^c(x), \end{aligned} \quad (41)$$

where, again, $\Delta_1^c(x)$ and $\Delta_2^c(x)$ represent the uncertainty terms.

We can define

$$\tilde{\zeta}(x, \mu) = b_c(x, \tilde{f}, \tilde{g}) + A_c(x, \tilde{f}, \tilde{g})\mu. \quad (42)$$

Then, the real value of the constraint can be expressed as

$$\zeta(x, \mu) = \tilde{\zeta}(x, \mu) + \Delta_1^c(x) + \Delta_2^c(x)\mu. \quad (43)$$

We can then build estimators of the form

$$\hat{\zeta}_{\theta}(x, \mu) = \tilde{\zeta}(x, \mu) + \beta_{\theta}^C(x) + \alpha_{\theta}^C(x)\mu, \quad (44)$$

with α_{θ}^C and β_{θ}^C being RL policy. The goal of the RL agent is again in this case to make the estimator $\hat{\zeta}_{\theta}$ as close as possible to ζ .

Expanding $\tilde{\zeta}$ we can rewrite the estimator as

$$\hat{\zeta}_{\theta}(x, \mu) = \underbrace{(b_c(x, \tilde{f}, \tilde{g}) + \beta_{\theta}^C(x))}_{b_{\theta}^C(x)} + \underbrace{(A_c(x, \tilde{f}, \tilde{g}) + \alpha_{\theta}^C(x))}_{A_{\theta}^C(x)} \mu. \quad (45)$$

And the final optimization problem, which includes the learned estimates of the uncertain terms is:

RL-CBF-CLF-QP:

$$\begin{aligned} \mu_{\theta}^*(x) &= \underset{\mu, \mu_b, d}{\operatorname{argmin}} \mu^T \mu + p d^2 \\ \text{s.t. } & \widehat{V}_{\varepsilon, \theta}(\eta, z, \mu) + \frac{\lambda}{\varepsilon} V_{\varepsilon}(\eta) \leq d \quad (\text{RL-CLF}) \\ \text{for } i &= 1 \cdots n_b \quad \mu_{b,i} + K_{b,i} \eta_{b,i}(x) \geq 0 \quad (\text{RL-CBF}) \\ & \mu_{b,i} = \widehat{B^{(r_b)}}_{i, \theta}(x, \mu) \\ \text{for } j &= 1 \cdots n_c \quad A_{\theta}^C(x)\mu + b_{\theta}^C(x) \leq 0 \quad (\text{RL-Constraints}) \end{aligned} \quad (46)$$

V. REINFORCEMENT LEARNING BASED FRAMEWORK

In this section, we present a unified RL framework that can learn the uncertainty terms in the CLF, CBF, and other dynamic constraints specified in the earlier sections as $\alpha_{\theta}^V, \alpha_{\theta}^B, \alpha_{\theta}^C, \beta_{\theta}^V, \beta_{\theta}^B, \beta_{\theta}^C$.

A diagram of this framework is illustrated in Fig. 1. The RL agent learns a policy, which is a combination of uncertainty terms in CLF, CBF and other dynamic constraints. These uncertainty terms are then added to the QP constraints as derived from the nominal model, resulting in the estimates of the actual true CLF, CBF, and dynamic constraint dynamics

of the plant. Using these estimates, the RL-CBF-CLF-QP optimization problem in which model uncertainty is addressed, is solved to obtain a control input.

The reward function of the learning problem has to be designed such that it minimizes the estimation errors of the policy. The time-wise loss function is then defined as:

$$\begin{aligned} l_{V,\theta} &:= \|\dot{V}_\varepsilon - \hat{V}_{\varepsilon,\theta}(x, \mu)\|^2 \\ l_{B,\theta} &:= \|B^{(r_b)} - \widehat{B^{(r_b)}}_\theta(x, \mu)\|^2 \\ l_{C,\theta} &:= \|\zeta - \hat{\zeta}_\theta(x, \mu)\|^2 \end{aligned} \quad (47)$$

It is important to note that the true plant's dynamics information is not used for computing the values of this loss function. We use explicit expressions for V_ε , B and ζ and compute the time-derivatives \dot{V}_ε , $B^{(r_b)}$ using numerical differentiation.

A canonical RL problem can be formulated, with the reward for a given state x defined as the weighted sum of the negative loss functions in addition to a user-specific failure-case penalty $-l_e : \mathbb{R}^n \rightarrow \mathbb{R}$:

$$R(x, \theta) = -w_v l_{V,\theta} - \sum_{i=1}^{n_b} w_{b,i} l_{B_i,\theta} - \sum_{j=1}^{n_{c1}} w_{c,j} l_{C_j,\theta} - l_e(x). \quad (48)$$

Here, n_b and n_c are the number of CBF and other dynamic constraints respectively.

The learning problem can be defined as:

$$\begin{aligned} \max_{\theta} \quad & \mathbb{E}_{x_0 \sim X_0, w \sim \mathcal{N}(0, \sigma^2)} \int_0^T R(x(\tau), u_\theta(\tau)) d\tau \\ \text{s.t.} \quad & \dot{x} = f(x) + g(x) \tilde{u}(x, \mu_\theta^*(x) + \omega) \end{aligned} \quad (49)$$

A discretized version of it can be solved using conventional RL algorithms.

Remark 5: While running training experiments or simulations, it is assumed that the robot operates under the true (uncertain) plant dynamics. We will later show in Section VII that the trained policy works well even when the true plant in the evaluation differs from the plant of the training environment.

VI. APPLICATION TO BIPEDAL ROBOTS

The goal of this section is to validate that the RL-CBF-CLF-QP framework enables safety-critical control even when model uncertainty is present.

We will validate our method on RABBIT (Chevallereau et al. [6]) (Fig. 2), a planar bipedal robot, walking on a discrete terrain of stepping stones.

A. Simulation Settings

We run mainly two simulation with our method, and offer comparisons with the previous methods. The first simulation consists of RABBIT simply walking on a flat terrain. We evaluate the CLF based methods in Section III in this settings. This is to verify only the stabilizing capacity of our proposed method under the model uncertainty. In the second simulation,

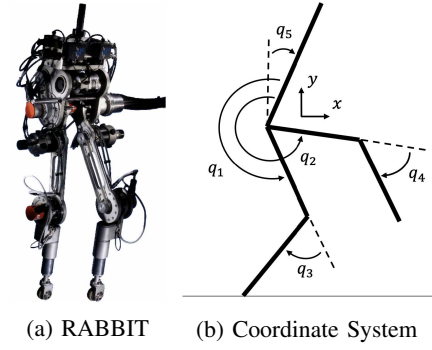


Fig. 2: RABBIT, a planar five-link bipedal robot. $q = [x, y, q_1, q_2, q_3, q_4, q_5]^T$

we put the robot on a discrete random stepping stone terrain (Fig.5). The robot's task here is to place the foot always on the stepping stone, while managing the stability and not violating the contact-force constraint. The full RL-CBF-CLF-QP is tested in this task.

The main model uncertainty in this demonstration is introduced by scaling all mass and inertia parameters of each link by a constant scale factor = 2, i.e. the nominal model's mass and inertia terms are half of the actual plant. During the training of the RL agent, it only has knowledge of the nominal model.

During the simulation, a single periodic walking gait trajectory, which is generated offline by Fast Robot Optimization and Simulation Toolkit (FROST) (Hereid and Ames [9]), is used. The output function $h(x)$ is defined as the difference between the actuated joint angles and the desired trajectory's joint angles. The gait's nominal step length is 0.35m. Finally, a torque saturation of 200Nm is applied to the control inputs of all simulations including training and evaluation.

B. Reinforcement Learning Settings

We train our agent using a standard Deep Deterministic Policy Gradient Algorithm (DDPG, Silver et al. [16]). DDPG is used to learn the parameters of the actor and critic neural networks. The input for the actor neural network is 14 observations, which is RABBIT's full state, in addition to the CBF parameter $-l_{min}$ —for the second simulation. The output dimension is 25, corresponding to $4 \times 1 \alpha_\theta^V, \alpha_{\theta,1}^B, \alpha_{\theta,2}^B, \alpha_{\theta,1}^C, \alpha_{\theta,2}^C$ and $1 \times 1 \beta_\theta^V, \beta_{\theta,1}^B, \beta_{\theta,2}^B, \beta_{\theta,1}^C, \beta_{\theta,2}^C$. Both actor and critic neural networks have two hidden layers of width 400 and 300. This agent is trained on the simulation of ten walking steps per episode, and a discrete time step $T_s = 0.01\text{sec}$ is used. The failure cases are determined by the robot's pose. The training environment used in this paper is on six multiple cores of Intel(R) Core(TM) i5-9400F CPU (2.90GHz) without the use of GPU, and it took about 34 seconds per episode for the training. The final agent in use is obtained after 79 and 133 episodes for RL-CLF-QP and RL-CBF-CLF-QP respectively.

VII. RESULTS

During the evaluation, the robot is tested on the uncertainty that is introduced in the training, but in addition to it, two other

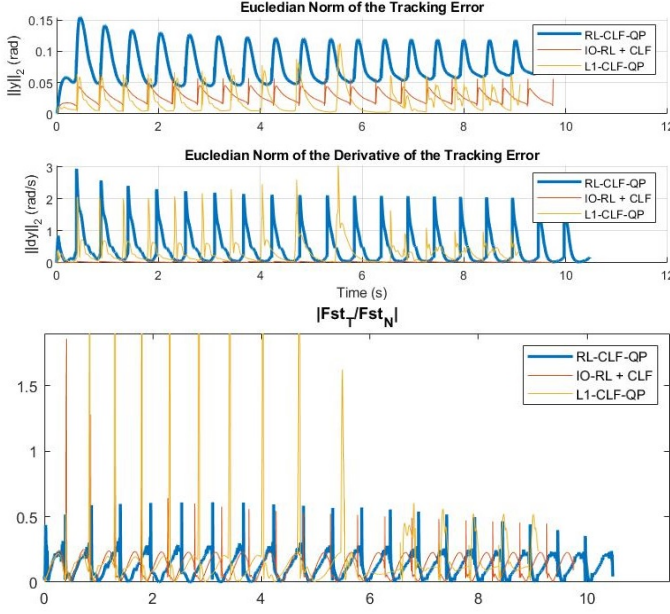


Fig. 3: Tracking error (top) and tangential-normal contact force ratio (bottom) of the three CLF-based controllers, simulated for twenty walking steps, where the robot's mass and inertia values are scaled by a factor of 2. Only the RL-CLF-QP satisfies $|F/N| \leq k_f = 0.8$

kinds of uncertainty are introduced. First, the robot's motor dynamics that restricts the change rate of joint torques are applied in every evaluation. The time constant of motors used in the simulation is 0.004. Second, the robot is also tested on an alternative kind of uncertainty, which is an added weight to the torso of a robot. This weight can represent a robot carrying a payload, and it is deliberately introduced to evaluate the trained policy's robustness to an unfamiliar kind of uncertainty.

A. Simulation 1: Bipedal Walking on Flat Ground

For the first simulation, we evaluate the two RL approaches for CLF, explained in Section III, and compare it with the standard L1 Adaptive CLF-QP Method of Nguyen and Sreenath [13], which guarantees the CLF to be bounded to a small value under model uncertainty if using a sufficiently large adaptation gain. From now on, we will call IO-RL+CLF the controller resulting from the approach of Section III-A and RL-CLF-QP the controller resulting from the approach of III-B.

As illustrated in Fig. 3, all three methods manage to get RABBIT to stably walk on multiple steps. Note that all three methods do not have friction constraint as part of the QP and could potentially violate the friction constraints. In particular, the RL-CLF-QP method succeeds in keeping the contact force under the friction constraint for all steps, the IO-RL+CLF exceeds the limit in the first step and L1-CLF-QP violates it for multiple steps. Note that the original CLF-QP from Section II-B fails under this scaled model uncertainty.

Displayed in Fig. 4 is the plot of tracking error and contact force ratio of the three controllers when, instead of the mass-inertia-scaling, an additional torso weight of 32kg (100% of

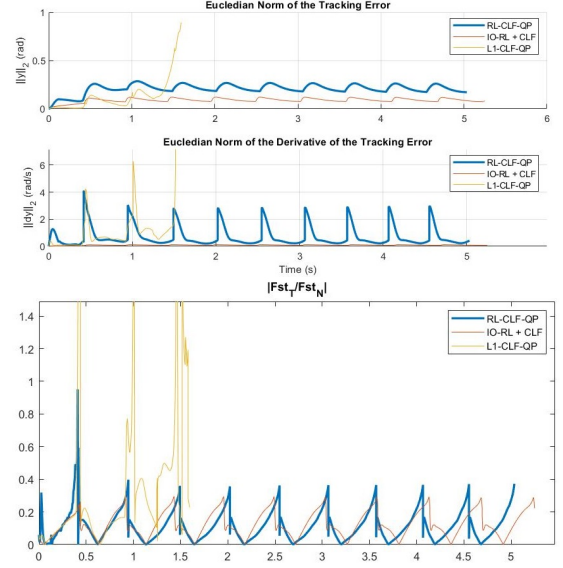


Fig. 4: Tracking error (top) and contact force ratio (bottom) of the three CLF-based controllers, simulated for ten walking steps with the additional torso weight 32kg (this amounts to the weight of RABBIT).

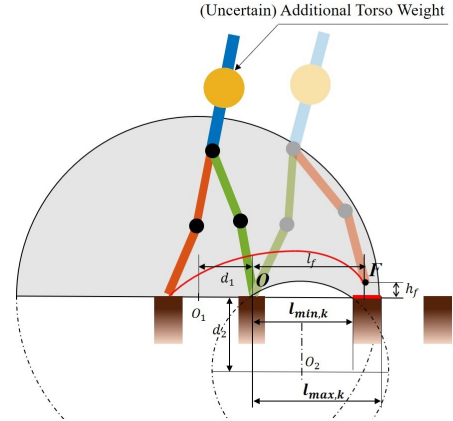


Fig. 5: Description of the safety constraints. They are defined during the entire walking step, forcing the swing foot to land on the stepping stone.

the robot mass) is introduced. It is notable that both the RL-CLF-QP and IO-RL+CLF manage to adapt to this uncertainty, which has not been faced during the training. The RL-CLF-QP violates the friction limit for 0.013 seconds near the end of the first step. Furthermore, the RL-CLF-QP manages to stabilize the walking gait with an additional torso weight of up to 72kg (225% of robot mass). On the other hand, IO-RL+CLF manages to adapt to the weight of 53kg (166% of robot mass).

B. Simulation 2: Bipedal Walking on Stepping Stones with One Step Preview

Having verified the stabilizing performance of both RL-CLF-QP and IO-RL+CLF methods in the first simulation,

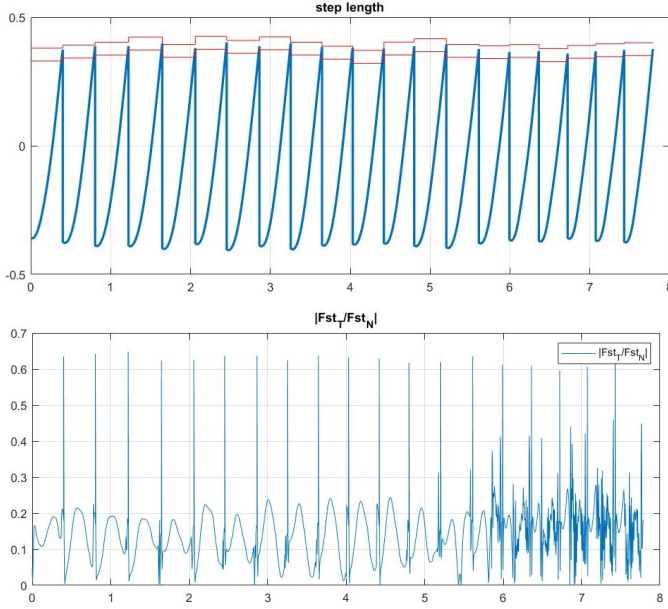


Fig. 6: Results of the simulation of walking 20 stepping stones, where the robot’s mass and inertia values are scaled by a factor of 2. (Top) History of swing foot position(l_f) for each step, where the stepping stone constraints(l_{min}, l_{max}) are plotted with the red lines. (Bottom) History of tangential-normal contact force ratio that satisfies to stay below $|F_T/F_N| \leq k_f = 0.8$

we now evaluate the full RL-CBF-CLF-QP method with the safety-critical constraint of walking on stepping stones. In this setting, for each step, a robot faces a random placement of a stepping stone. When the swing foot hits the ground at the end of the step, we want the step length to be within a specific range:

$$l_{min,k} \leq l_k \leq l_{max,k}, \quad (50)$$

where k indicates the step index. Two position-constraints-based second order ECBFs parameterized by $l_{min,k}, l_{max,k}$ that are a sufficient condition for (50) are devised by Nguyen and Sreenath [12]. Basically these constraints imply that the swing foot position (F in Fig.5) needs to stay within the grey area. Note that $l_{min,k}, l_{max,k}$ changes for every step.

We also include contact force constraints in the RL-CBF-CLF-QP. These are important, since for the case of walking on stepping stones, the original CBF-CLF-QP tends to violate the friction cone and the unilaterality of normal forces repeatedly. Contact forces are linear on the inputs but depend on the dynamics of the system, so RL will need to be used for addressing the uncertainty in the contact force constraints.

During the training, under the model uncertainty, the robot is trained to walk on randomly spaced stepping stones, of which l_{min} is sampled from a normal distribution $\mathcal{N}(\mu = 0.35m, \sigma = 0.02m)$, truncated at 2.5σ . l_{max} is set as $l_{min} + 0.05m$.

Fig.6 shows the result of the evaluation, where the robot walks on 20 randomly spaced stepping stones. The sample

distribution of l_{min} here is same as in the training. Readers can check that the foot placement is always on the stepping stones. Also, it is verified that the contact force never exceeds the friction limit.

Whereas our RL-CBF-CLF-QP method performs well, we have also tested the original CBF-CLF-QP method in Section II-C on this simulation for comparison. The CBF-CLF-QP is also solved together with the friction constraints. However, it violates the step length safety constraints after an average of 5.6 ± 4.64 steps. This value is obtained from 10 random executions of 20 steps simulation.

Our method even manages to walk on the stepping stones sampled from higher variance distributions of l_{min} . We have tested the limit of our trained agent on where l_{min} is sampled from uniform distributions of $[l_l, l_u]$ for ten steps. We considered violating either safety or friction constraints for more than one step during the simulation as failure. The success limit in terms of never violating the friction constraint as well as the safety constraint is $l_l = 0.31m, l_u = 0.42m$, slightly bigger than the training environment’s l_{min} sampling range.

Finally, under the additional torso weight applied to the original scale plant, RL-CBF-CLF-QP still manages to stay within the safety and friction constraints for the weight in the range of [43kg, 72kg] (134-225% of robot mass).

VIII. DISCUSSION

In Sections VI and VII, we have demonstrated that our method of safety-critical control adapts well for trained model uncertainty, and also shows some robustness in introduction of different kinds of model uncertainty. However, a primary drawback is that we need the designed nominal controller to not rapidly fail on the uncertain system before the RL can learn the uncertainty. For instance, for our application of bipedal walking, we need the nominal controller to be able to take a significant part of a step. This may not always be possible depending on the level of uncertainty. Additionally, it must be noted that we do not have theoretical guarantees on feasibility of the CBF-CLF-QP.

IX. CONCLUSION

We have addressed the issue of model uncertainty in safety-critical control with a RL-based data-driven approach. We have presented a formal analysis of uncertainty terms in CBF and CLF constraints, in addition to other dynamic constraints. Our framework includes two core components: 1) an RL agent which learns to reduce the model uncertainty in the aforementioned safety constraints, and 2) the formulation of the RL-CBF-CLF-QP problem that solves online for the safety-critical control with the adjusted safety constraints. The proposed framework is tested on RABBIT, an underactuated nonlinear bipedal robot, walking on randomly spaced stepping stones with one step preview.

REFERENCES

- [1] A. D. Ames and M. Powell. Towards the unification of locomotion and manipulation through control lyapunov

- functions and quadratic programs. In *Control of Cyber-Physical Systems*, pages 219–240. Springer, 2013.
- [2] A. D. Ames, K. Galloway, K. Sreenath, and J. W. Grizzle. Rapidly exponentially stabilizing control lyapunov functions and hybrid zero dynamics. *IEEE Transactions on Automatic Control*, 59(4):876–891, April 2014. ISSN 2334-3303. doi: 10.1109/TAC.2014.2299335. URL <https://ieeexplore.ieee.org/document/6709752>.
 - [3] A. D. Ames, J. W. Grizzle, and P. Tabuada. Control barrier function based quadratic programs with application to adaptive cruise control. In *53rd IEEE Conference on Decision and Control*, pages 6271–6278, Dec 2014. doi: 10.1109/CDC.2014.7040372.
 - [4] S. Bansal, R. Calandra, T. Xiao, S. Levine, and C. J. Tomlin. Goal-driven dynamics learning via bayesian optimization. In *2017 IEEE 56th Annual Conference on Decision and Control (CDC)*, pages 5168–5173, Dec 2017. doi: 10.1109/CDC.2017.8264425.
 - [5] F. Berkenkamp, M. Turchetta, A. Schoellig, and A. Krause. Safe model-based reinforcement learning with stability guarantees. In *Advances in neural information processing systems*, pages 908–918, 2017.
 - [6] C. Chevallereau, G. Abba, Y. Aoustin, F. Plestan, E. R. Westervelt, C. Canudas-De-Wit, and J. W. Grizzle. Rabbit: a testbed for advanced control theory. *IEEE Control Systems Magazine*, 23(5):57–79, 2003.
 - [7] J. F. Fisac, A. K. Akametalu, M. N. Zeilinger, S. Kaynama, J. Gillula, and C. J. Tomlin. A general safety framework for learning-based control in uncertain robotic systems. *IEEE Transactions on Automatic Control*, 64(7):2737–2752, July 2019. ISSN 2334-3303. doi: 10.1109/TAC.2018.2876389. URL <https://ieeexplore.ieee.org/abstract/document/8493361>.
 - [8] K. Galloway, K. Sreenath, A. D. Ames, and J. W. Grizzle. Torque saturation in bipedal robotic walking through control lyapunov function-based quadratic programs. *IEEE Access*, 3:323–332, 2015. ISSN 2169-3536. doi: 10.1109/ACCESS.2015.2419630.
 - [9] A. Hereid and A. D. Ames. Frost: Fast robot optimization and simulation toolkit. In *2017 IEEE/RSJ International Conference on Intelligent Robots and Systems (IROS)*, pages 719–726. IEEE, 2017. URL <https://ieeexplore.ieee.org/document/8202230/definitions>.
 - [10] J. Hwangbo, J. Lee, A. Dosovitskiy, D. Bellicoso, V. Tsounis, V. Koltun, and M. Hutter. Learning agile and dynamic motor skills for legged robots. *Science Robotics*, 4(26):eaau5872, 2019.
 - [11] S. Levine, C. Finn, T. Darrell, and P. Abbeel. End-to-end training of deep visuomotor policies. *J. Mach. Learn. Res.*, 17(1):13341373, January 2016. ISSN 1532-4435.
 - [12] Q. Nguyen and K. Sreenath. Optimal Robust Time-Varying Safety-Critical Control With Application to Dynamic Walking on Moving Stepping Stones. In *ASME 2016 Dynamic Systems and Control Conference*. American Society of Mechanical Engineers Digital Collection. URL <https://asmedigitalcollection.asme.org/DSCC/proceedings-abstract/DSCC2016/50701/V002T28A005/231011>.
 - [13] Q. Nguyen and K. Sreenath. L1 adaptive control for bipedal robots with control lyapunov function based quadratic programs. In *2015 American Control Conference (ACC)*, pages 862–867, July 2015. doi: 10.1109/ACC.2015.7170842. URL <https://ieeexplore.ieee.org/document/7170842>.
 - [14] Q. Nguyen and K. Sreenath. Exponential control barrier functions for enforcing high relative-degree safety-critical constraints. In *2016 American Control Conference (ACC)*, pages 322–328, July 2016. doi: 10.1109/ACC.2016.7524935. URL <https://ieeexplore.ieee.org/document/7524935>.
 - [15] S. Sastry. *Nonlinear systems: analysis, stability, and control*. Vol. 10. Springer Science and Business Media, 1999. URL <https://www.springer.com/gp/book/9780387985138>.
 - [16] David Silver, Guy Lever, Nicolas Heess, Thomas Degris, Daan Wierstra, and Martin Riedmiller. Deterministic policy gradient algorithms. 2014.
 - [17] A. J. Taylor, V. D. Dorobantu, H. M. Le, Y. Yue, and A. D. Ames. Episodic learning with control lyapunov functions for uncertain robotic systems. *arXiv preprint arXiv:1903.01577*, 2019. URL <https://arxiv.org/abs/1903.01577>.
 - [18] A. J. Taylor, A. Singletary, Y. Yue, and A. D. Ames. Learning for safety-critical control with control barrier functions. *arXiv preprint arXiv:1912.10099*, 2019. URL <https://arxiv.org/abs/1912.10099>.
 - [19] T. Westenbroek, D. Fridovich-Keil, E. Mazumdar, S. Arora, V. Prabhu, S. S. Sastry, and C. J. Tomlin. Feedback linearization for unknown systems via reinforcement learning. *arXiv preprint arXiv:1910.13272*, 2019. URL <https://arxiv.org/abs/1910.13272>.